Panoramic Camera Calibration
Using 3D Straight Lines

Jafar Amiri Parian, Armin Gruen

Institute of Geodesy and Photogrammetry
Swiss Federal Institute of Technology (ETH) Zurich
(parian, agruen)@@geod.baug.ethz.ch

KEY WORDS: Panoramic Camera, Calibration, Straight Line Feature, Multi-Projection Center Image, Accuracy Test.

ABSTRACT:

Linear array CCD - based panoramic cameras are being used for measurement applications. The elegant image acquisition mode and the high information content of those images make them suitable candidates for quantitative image analysis. For accurate measurements a sophisticated camera calibration is an important prerequisite. In our previous investigations we designed a sensor model for linear array CCD - based rotating panoramic cameras, which models substantial deviations from the pinhole model using additional parameters. The additional parameters are related to the camera itself, the configuration of camera, the turntable, and mechanical errors of the camera system during rotation (i.e. tumbling). We measured the tumbling of the SpheroCam by an inclinometer and also modeled tumbling in connection with the collinearity equations. We showed a subpixel level accuracy after tumbling modeling. Determining tumbling parameters with bundle adjustment needs many control points and this makes the use of this sensor a bit inconvenient. Using existing object space information, such as 3D straight lines can provide extra conditions for reducing the number of control points for calibration and orientation. So far straight line information has been mainly used for determining interior orientation and additional parameters with single frame cameras. Due to the eccentricity of the projection center from the rotation axis the acquired panoramic images do not have a single projection center. Therefore the formulations which have been used for single projection center cameras cannot be applied in this case.

In this paper we give a new formulation for the processing of 3D straight lines in panoramic cameras. We show how 3D straight line information can be used in addition to tie points for calibration and orientation. We will present the results of our new investigations by using 3D straight lines as stochastic constraints in the bundle system for determining the tumbling parameters in addition to the other additional parameters. This allows us to do a full calibration and orientation without control points, which makes the use of the sensor more efficient.

1. INTRODUCTION

With the development of digital technology, a new generation of dynamic rotating panoramic cameras was introduced. The principle of the operation is the same as with analogue rotating panoramic cameras. The imaging sensor is a CCD line, which is mounted on a turntable parallel to the rotation axis. A large linear array provides a large format size for the final image. The EYESCAN, jointly developed by German Aerospace Center (DLR) and KST Dresden GmbH and the SpheroCam, SpheronVR AG are two different products of linear array-based panoramic cameras.

The EYESCAN camera as used in terrestrial photogrammetric applications was addressed in Scheibe et al., 2001. Schneider and Maas, 2003 and Amiri Parian and Gruen, 2004 have worked on the mathematical modeling of linear array-based panoramic cameras. Schneider and Maas, 2003 investigated a geometrical model for a prototype of the EYESCAN and they performed calibration by using a 3D testfield. They also performed 3D positioning using bundle block adjustment (Schneider and Maas, 2004). We worked on the mathematical model of general linear array-based panoramic cameras. We performed calibration and accuracy tests using a 3D testfield for the EYESCAN and the SpheroCam (Amiri Parian and Gruen, 2003). We improved the mathematical model by modeling the mechanical errors of the rotating turntable, e.g. the tumbling,

and we reported a subpixel level of accuracy and the improvement of the accuracy by a factor of two in the case of using tumbling parameters in the bundle adjustment process (Amiri Parian and Gruen, 2004a). We investigated the minimal number of control points for selfcalibration and showed that with 3 control points selfcalibration is possible provided that the additional parameters of the mechanical errors are available in advance (Amiri Parian and Gruen, 2004b). We estimated the additional parameters which are related to mechanical errors by selfcalibration using many control points. However this is not practical in real projects. One solution could be to use object space constraints such as straight lines.

Straight line features in camera calibration procedures have been used by Brown, 1971 who introduced the plumb-line method. Straight lines were used to derive symmetrical radial and decentering lens distortions. The principle behind this method is that the straightness of the lines in object space should be preserved in image space by perspective projection if an ideal camera is considered. Deviations of the projected straight line in image space are modeled by respective additional parameters which are mainly symmetrical radial and decentering lens distortion parameters. Kager and Kraus, 1976 incorporated geometric constraints such as lines, coordinate differences, horizontal and space distances, different lines of planes and angles to improve the traditional bundle adjustment method. Hell, 1979 proposed line constraints and used it in the

form of coplanarity conditions in the bundle adjustment. Heuvel, 1999 used parallel and perpendicular straight lines and estimated in addition to radial lens distortion parameters other parameters: shift of principal point and focal length (interior orientation parameters). Habib et al., 2004 investigated the possibility of using straight lines for calibration and orientation. They used directly the model of 3D straight lines in object space.

After our investigation on sensor modeling and accuracy tests we are also interested in to do camera calibration with no control points at all or without using more control points than needed for minimal constraints datum definition by means of 3D straight line information.

2. PANORAMIC IMAGING

Several techniques have been used for panoramic imaging. Mosaicking/stitching of a rotated frame-CCD camera, mirror technology including single mirror and multi mirrors, near 180 degrees with large frame cameras or one shot with fish-eye lens and recently a new technology of creating high resolution panoramic images by rotating a line-CCD camera are some known methods for panoramic imaging. Up to now, these techniques have mainly been used for pure imaging purposes, such as indoor imaging, landscape and cultural heritage recording, tourism, advertising, image-based rendering, and recently for efficient Internet representations. However, some of these techniques are used in computer and robot vision for navigation applications due to the large field of view, but none of them is used for precise measurements and efficient 3D reconstruction.

Among the mentioned techniques for panoramic imaging, the linear array-based panoramic camera has the possibility to produce a high-resolution panoramic image (more than 300 Mpixels) in one turn. The camera principle of this technique consists of a linear array, which is mounted on a high precision turntable parallel to the rotation axis. By rotation of the turntable, the linear array sensor captures the scenery as a continuous set of vertical scan lines. In this investigation we used the SpheroCam from SpheronVR AG. In previous works (Amiri Parian and Gruen 2003, 2004a, 2004b) we have also used and calibrated the SpheroCam.

2.1. SpheroCam

The structure of the SpheroCam (Figure 1) includes three parts: a camera head, an optical part which is compatible with NIKON-lenses, and a DC motor to rotate the linear array. The SpheroCam is specially designed for use with a fish-eye lens, which has a near 180° vertical field of view. When it rotates around its vertical axis, it captures a complete spherical image. The linear array consists of 5300 pixels. It scans 39270 columns during one rotation with a 50-mm lens. The final image has approximately 200 Mpixels resolution. For more details on specifications of the camera see Amiri Parian and Gruen, 2003 and 2004a.

3. SENSOR MODEL

For the sake of simplicity of the formulations, we have defined four coordinate systems as follows:

1. Pixel coordinate system
2. Linear array coordinate system
3. 3D auxiliary coordinate system
4. 3D object coordinate system

Figure 2 shows these coordinate systems and Figure 3 the pixel coordinate (i, j) system in which the original image observations are stored.

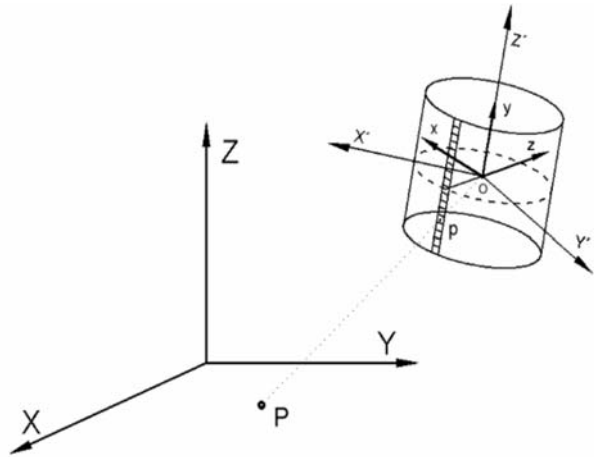Figure 1. The digital terrestrial panoramic camera SpheroCam.

Figure 2. The object coordinate (X, Y, Z), auxiliary coordinate (X', Y', Z') and linear array (x, y, z) coordinate systems.
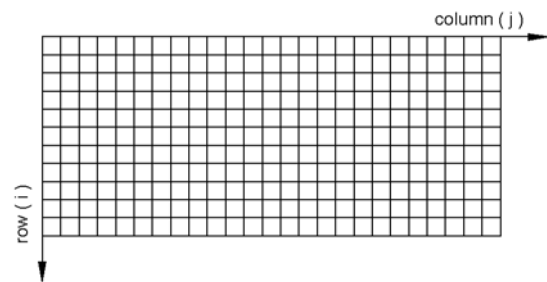

Figure 3. The pixel coordinate system (i, j).

The functional model for an ideal sensor (Amiri Parian and Gruen, 2003), which shows principally the relation of the four coordinate systems to each other, becomes:

$$\begin{pmatrix} 0 \\ y \\ -c \end{pmatrix} = \lambda\, P^{-1}\, R_z^t\, (j\, A_h)\, M_{w,\varphi,k} \begin{pmatrix} X - X_O \\ Y - Y_O \\ Z - Z_O \end{pmatrix} \quad (1)$$

With

$$P = \begin{pmatrix} 0 & 0 & -1 \\ -1 & 0 & 0 \\ 0 & 1 & 0 \end{pmatrix} \qquad y = (i - \frac{N}{2}) A_v$$
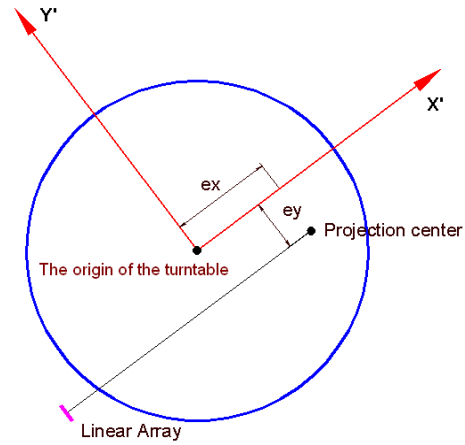
where,

A_h	Resolution of rotation
A_v	The pixel size of the linear array
c	Camera constant
N	The number of rows or number of pixels in the linear array
R_z	3D rotation matrix around Z axis
P	Transformation matrix. From the linear array to the auxiliary coordinate system
$(x, y, -c)$	Coordinates of image points in the linear array coordinate system
λ	Scale factor
$M_{w,\varphi,k}$	Rotation matrix
(X_0, Y_0, Z_0)	Location of the origin of the auxiliary coordinate system in the object space coordinate system

Systematic errors will disturb the ideal sensor model. For the linear array-based panoramic cameras the most important ones with a distinct physical meaning are:
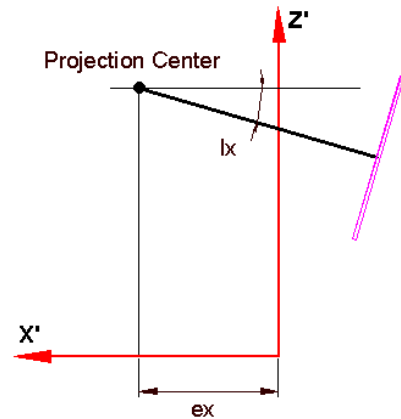
1. Lens distortion
2. Shift of principal point
3. Camera constant
4. Tilt and inclination of the linear array with respect to the rotation axis
5. Eccentricity of the projection center from the origin of the auxiliary coordinate system
6. Resolution of rotation
7. Mechanical errors of turntable during rotation, including tumbling and uneven rotation of the turntable

We formulated additional parameters for the modeling of the systematic errors and added them to the sensor model. They can be divided into four different groups. The first is related to the camera head and optics (parameters of classes 1, 2 and 3). The second group of parameters (Figure 4) is related to the configuration of the camera head and the plane of the turntable (parameters of classes 4 and 5). The third group is related to the turntable itself (the parameter of class 6). The fourth group refers to the mechanical errors of the turntable, tumbling, while the camera rotates (parameters of class 7).
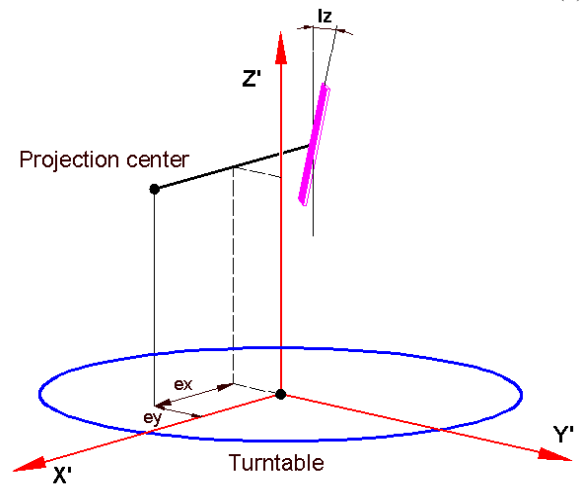
One of the main systematic errors of the camera system is tumbling, resulting from the mechanical properties of the instrument and mainly caused by an incomplete shape of ball bearings and the contacting surfaces (Matthias, 1961). It is affected by the rotation around the vertical axis and shows its effect as a change of the exterior orientation of the camera head during rotation. One of the main effects of the tumbling is the moving of the origin of the auxiliary coordinate system during rotation (Figure 5). For more detailed information on the mathematical modeling of the tumbling see Amiri Parian and Gruen, 2004a.

(a)

(b)

(c)

Figure 4. Additional parameters of the configuration of the camera on the turntable. (a) Eccentricity (ex, ey), (b) the tilt of the linear array (lx), (c) the inclination of the linear array with respect to the rotation axis (lz).
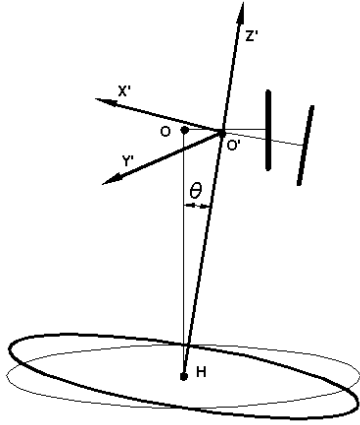
Figure 5. The effect of tumbling: The movement of the origin of the auxiliary coordinate system.

4. STRAIGHT LINE MODELING

The straight line modeling for the case of concentric panoramic cameras is the same as the case of single-projection center cameras. This case has been already studied in Habib et al., 2000. We used the same concept but applied another formulation with the advantage that we define a weight for each constraint. Each constraint can be treated as a stochastic condition equation. This gives ability to compensate any small deviation of the 3D straight line from straightness by adjusting the weights.

A 3D straight line in object space is defined by two distinct points A and B (Figure 6). These points are the intersected rays of the corresponding points in different images. For example, the ray intersection of the image point a1 and a2 is an object point A. In the case of an ideal panoramic camera (concentric and with no systematic errors) the projected 3D straight line is cylindrical section (a part of circle or ellipse) and for the ideal single frame camera it is a straight line. The intermediate rays ($\vec{V}$) of the segment line AB should be coplanar with the plane defined by $\vec{V_1}$ and $\vec{V_2}$ (Figure 7). The coplanarity is formulated:

$$(\vec{V_1} \times \vec{V_2}) \cdot \vec{V} = 0 \qquad (2)$$

In which $\times$ and $\cdot$ are cross and inner (dot) products respectively. We give another formulation in form of equation (3), which formulates the distance of a point from a plane.

$$s = \frac{|aX + bY + cZ - d|}{\sqrt{a^2 + b^2 + c^2}} \qquad (3)$$

In which $| \ |$ stands for the absolute value,

a, b, c, d .... Parameters of the plane defined by $\vec{V_1}$ and $\vec{V_2}$. The first three parameters are the elements of the normal to the plane. The plane equation is $aX + bY + cZ = d$.

X, Y, Z ..... Coordinates of $\vec{V}$.

s .... Distance of the image point from the plane which is defined by $\vec{V_1}$ and $\vec{V_2}$.

Equation (3) can be treated as an observation equation and in the optimization procedure s should be minimized. The deviation of the 3D straight line from the straightness and the precision of the image line observations together can be defined as the precision of s. This will define the initial weight value and better weights can be estimated after adjustment by computing the cofactor matrix of the adjusted observations.

These equations cannot be applied to multi-perspective center images, for example to a panoramic camera with large eccentricities of the projection center. In these cases the incoming rays of the 3D straight line span a surface which is not a plane. Figure 8 shows this surface. The projected 3D straight lines in image space in this case produce a modulated sine wave function.
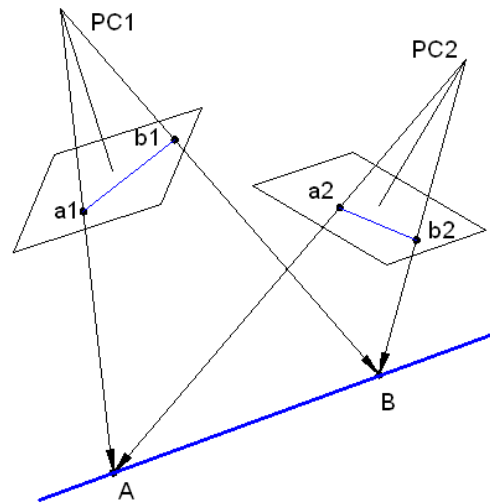

Figure 6. Defining a straight line by the intersection of rays of two distinct corresponding points in different images. The projection centers of the images are denoted by PC1 and PC2.
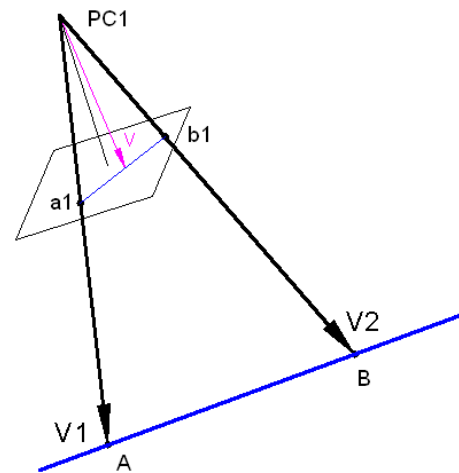

Figure 7. Coplanarity condition, the concept of the modeling 3D straight line for single frame and concentric panoramic cameras.
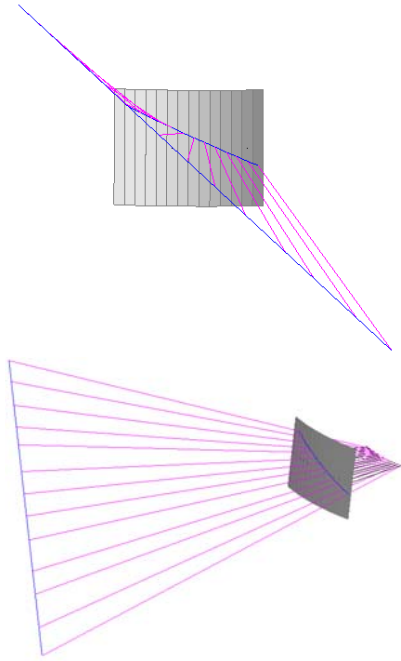
Figure 8. Multi-projection center images. Two different views of the projected 3D straight line in image space. The imaged line is a part of a modulated sine wave function. The surface created by the rays of the 3D straight line is not a plane.
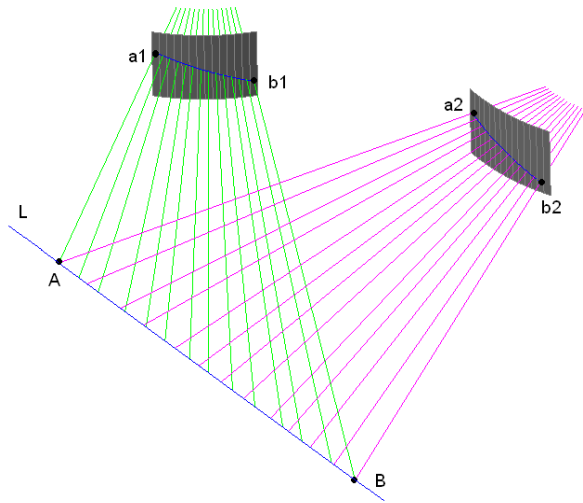

Figure 9. Defining a 3D straight line L by the intersection rays of two distinct corresponding points in different panoramic images.

Similar to the previous definition of a 3D straight line, for the case of multi-projection center images a 3D straight line is defined based on the intersection rays of two distinct corresponding points in image space (Figure 9).

The mathematical model of 3D straight line is based on the Euclidian distance, the same as equation (3). In this case the minimum distance of the lines Li and L (see Figure 10) defines the stochastical condition equation (4). Inclusion of the equation (4) with other observation equations in the Least Squares adjustment procedure gives the solution.
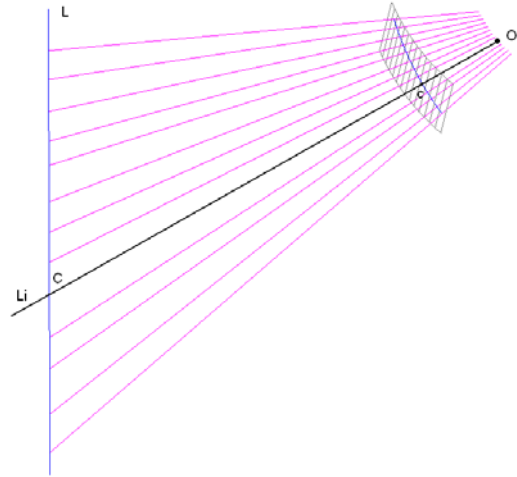
$$s = minimum\ distance\ (L,\ Li) \qquad (4)$$

Figure 10. Minimum Euclidian distance of Li and L, the concept of modeling the 3D straight line for multi-projection center images. The line Li is defined by O and c. O is the location of the projection center. C is a point on the 3D straight line and c is the image of C (O, C and c are collinear). See Figure 9 for the definition of the 3D straight line L.

For the formulation of equation (4) the weights can be defined based on the accuracy of the image line measurements and the deviations from a 3D perfect straight line.

We examined both formulations for panoramic cameras and in the next section we report the result of the 3D straight line modeling based on equation (4).

5. RESULTS

We show the effects of mechanical errors, especially the tumbling. We also analyze the effect of tumbling modeling in object space by an accuracy test. Then we use 3D straight line constraints in addition to tie points for estimating all additional parameters including tumbling parameters, in a joint bundle adjustment procedure.

5.1. Camera calibration for SpheroCam

The camera calibration was performed using a testfield (Figure 11) with specifications given in Table 1. We established a testfield with 96 circular targets at our Institute and used it for the calibration of the SpheroCam. The testfield was measured with a Theodolite with mean precision of 0.3, 0.3, 0.1 mm for the three coordinate axes (X, Y, Z). The camera calibration was performed by the additional parameters mentioned in chapter 3.

For the analysis of the additional parameters (to find the most influential parameters and those which are stable under the given network condition) we added step by step each parameter to the previous stage of the calibration and used the correlations for the stability checking. Table 2 shows the results of the selfcalibration after step by step adding additional parameters to the model.

In the last step, 3 parameters were used for tumbling modeling and 3 parameters for an uneven rotation modeling of the turntable (the tumbling and uneven rotation were modeled by sine curve functions with three parameters for each one: amplitude, period and phase). The a posteriori variance of unit

weight at the final level is 0.65 pixel (5.2 microns). It shows an improvement of the model by a factor of 2 with respect to the previous step of selfcalibration (without mechanical errors modeling).

Table 1. Specifications of the panoramic camera testfield

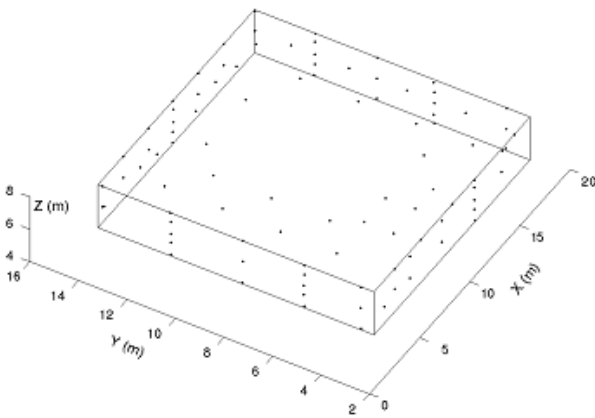| Measurement instrument	Theodolite (TC2002)
Number of control points	96
Dimension of the network (X, Y, Z)	15, 12, 3 (meters)
Mean/Max STD of control points (X,Y,Z)	0.3/0.9, 0.3/0.8, 0.1/0.3 (mm)
Depth and lateral precision	0.32, 0.22 (mm)

Figure 11. A 3D testfield for the calibration of panoramic cameras.
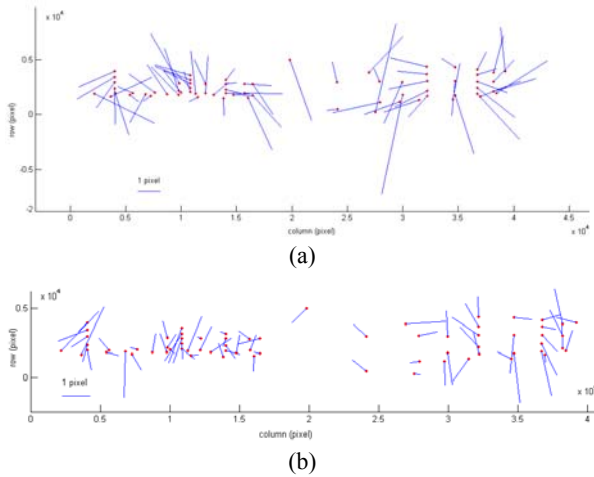

(a)

(b)

Figure 12. Image space residuals of image point observations. (a) Without tumbling modeling and (b) with tumbling modeling.

Figure 12 shows the image point residuals in image space for the two last steps of selfcalibration. However, the systematic patterns of the residuals has not been completely removed in the last step, but the size of the residual vectors are significantly reduced. The remaining systematic errors are due to non-modeled mechanical errors of the camera.

Table 2. Effect of additional parameters to the sensor model.

Parameters	$\hat{\sigma}_0$ [pixel]
Exterior orientation (6 parameters)	184.4
Resolution of rotation (1 parameter)	11.4
Camera constant, the shift of principal point and radial lens distortion (4 parameters)	2.5
Eccentricity of projection center (1 parameter)	2.0
Configuration of linear array with respect to turntable (3 parameters)	1.3
Tumbling and uneven rotation modeling (6 parameters)	0.65

5.2. Accuracy test

An accuracy test was performed for SpheroCam by block triangulation using 4 camera stations. The datum was defined by the inner constraints method using 87 control points using the same points as checkpoints.

Figure 13 shows the fitting accuracy of checkpoints. The pattern of residuals in object space shows a systematic trend and an incomplete sensor modeling. The reason is that the mathematical model cannot interpret the physical behavior of the dynamic camera system. To show the effect of the mechanical errors modeling, the tumbling and uneven rotation of the turntable parameters were added to the sensor model and the accuracy test was performed under the same conditions. The tumbling parameters in this case were computed in advance by bundle adjustment and using all available control points. Comparison of these parameters from 4 different camera stations implies that none of the parameters is block-invariant. However, some of them are close to be block-invariant, especially the periods of sine curve functions.

The summary of the adjustment results is in Table 3 for both mentioned cases. The RMS error from checkpoints before tumbling modeling are 9.9, 10.1 and 2.5 mm and with comparison to the standard deviations are too large. After tumbling modeling the RMS error of checkpoints are 1.7, 1.5 and 0.8 mm for X, Y and Z coordinate axes, which are in good agreement with the standard deviations, and show the effect of the mechanical errors modeling. Compared to the case when mechanical errors were not modeled we see an improvement of the accuracy by a factor of more than 4, especially for the depth (X and Y) axes.

Table 3. Results of accuracy test

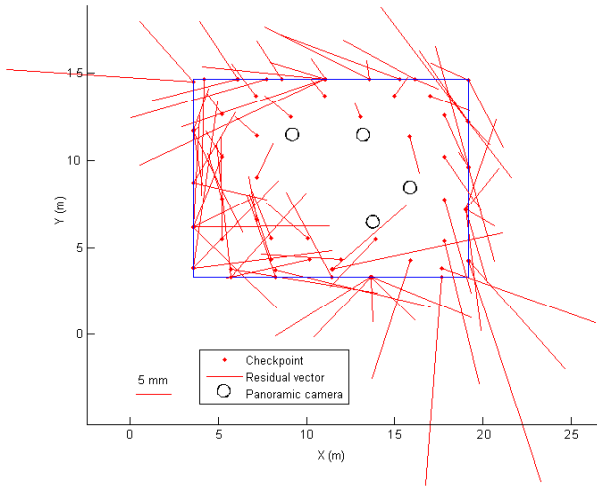| Number of control/checkpoints	87
Before tumbling modeling	
RMSE from checkpoints (X,Y,Z) (mm)	9.9, 10.1, 2.5
STD of checkpoints (X,Y,Z) (mm)	3.4, 2.7, 1.2
After tumbling modeling	
RMSE from checkpoints (X,Y,Z) (mm)	1.7, 1.5, 0.8
STD of checkpoints (X,Y,Z) (mm)	1.3, 1.1, 0.4

Figure 13. Residuals of checkpoints in object space (fitting accuracy) without tumbling modeling.
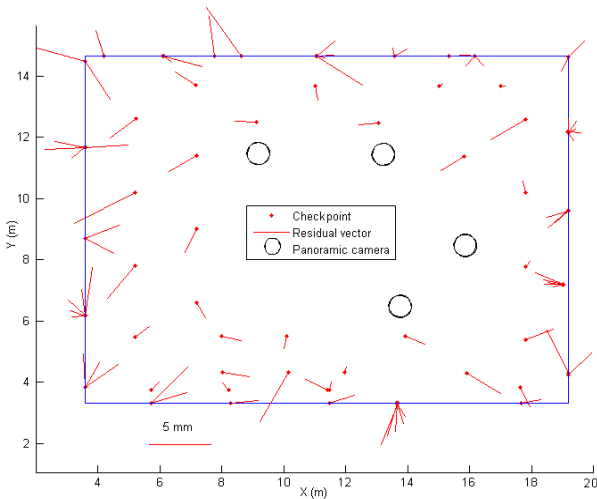

Figure 14. Residuals of checkpoints in object space (fitting accuracy) after tumbling modeling.

Figure 14 shows the object space residuals for checkpoints along the depth (X and Y) axes. By comparison of this Figure with Figure 13, the effect of the mechanical error modeling on removing the systematic errors is obvious. However, some local systematic errors can still be seen in the object space residuals.

5.3. Block adjustment and accuracy test using 3D straight line constraints

Due to the instability of the normal equations system of the bundle block adjustment, the parameters of the mechanical errors of the turntable cannot be estimated based on minimal constraints datum. In this part we show how by adding extra constraints to the observation equations of the sensor model these parameters can be estimated with minimal constraints datum. For the accuracy test we defined the datum with inner constraints using all available control points. We use the same images as under section 5.3.

The additional constraints that we use are 3D straight lines. The observations of the 3D straight lines were provided by existing features in the workspace area. In this investigation we used for example the borders of the existing desks to define 3D straight lines in object space (Figure 15). Assuming the ideal panoramic sensor, the projected straight lines should be a part of modulated sine curve function, since the geometry of the image is cylindrical. Any deviation of the projected straight line in the image space from the sine curve function should be modeled by additional parameters. The borders of the desks in the images were measured by subpixel precision after chaining the extracted edges by a Canny edge detector (Figure 16).

The corresponding edge points in image space were recovered by intersecting the related straight line edge segments. These points were introduced as new points in the bundle block adjustment for defining the 3D straight line in the object space.

The bundle block adjustment was performed with inner constraints datum. 87 checkpoints are available for accuracy analysis. 2 parameters (periods of sine curve functions) out of 6 parameters which model the mechanical errors of the turntable were considered as block-invariant parameters. 8 straight lines in object space were defined to be used as constraints and measured in 4 panoramic images. The average length of the projected straight lines in the images is 400 pixels.
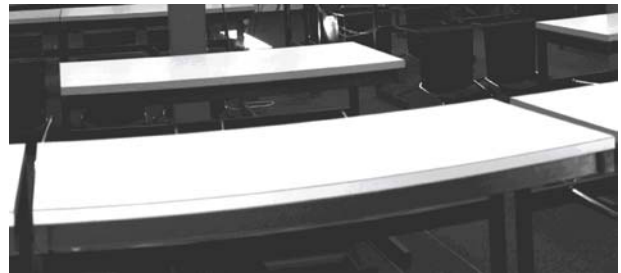

Figure 15. Borders of the desks were used as 3D straight lines in object space.
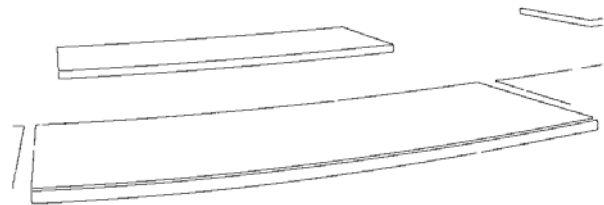

Figure 16. Extracted edges (subpixel) of borders of the desks after removing extra edges.

Table 4 shows the summary of the bundle adjustment computation. The RMS error from checkpoints compared with respect to RMS errors of Table 3 shows that the estimation of additional parameters was done successfully. However, there are some differences between the RMS values in Table 3 (after the tumbling modeling) and Table 4. Because we assumed that 2 parameters of the mechanical errors modeling (periods of sine curve functions) are block-invariant parameters whereas, as mentioned in the previous section they are not block-invariant. Due to the instability of the adjustment computation it was not possible to define those parameters as separate parameters for each image. Figure 17 shows the 3D straight lines which were used as constraints and the fitting accuracy of checkpoints in the object space.

Table 4. Bundle adjustment using 3D straight lines in addition to tie points (datum via inner constraints)

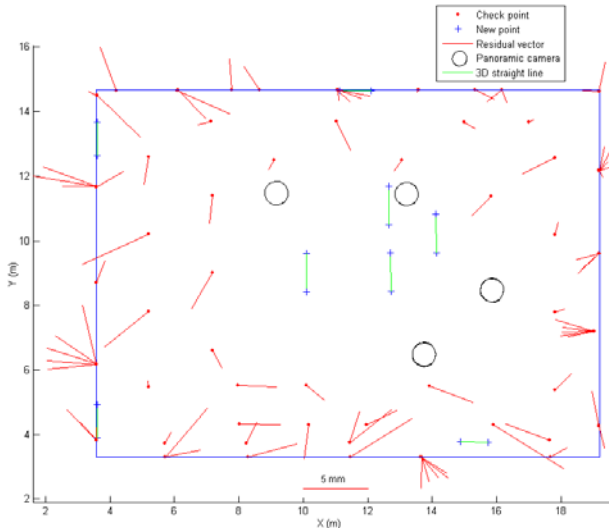| Number of checkpoints	87
Number of 3D straight lines	8
RMSE from checkpoints (X,Y,Z) (mm)	2.2, 1.6, 0.9
STD of checkpoints (X,Y,Z) (mm)	1.0, 0.8, 0.3

Figure 17. Residuals of checkpoints in object space (fitting accuracy). In this case the mechanical parameters of the turntable including tumbling parameters were estimated by bundle adjustment.

6. CONCLUSIONS

We gave a new formulation for the modeling of 3D straight lines as stochastic condition equations in bundle block adjustment for multi-projection center images. The formulation is in general form and can be applied to every camera of the same kind.

According to our results, orientation, calibration and accuracy test were performed successfully. All the additional parameters, especially the mechanically induced parameters (tumbling) of the panoramic camera were estimated successfully with the exception that 2 parameters (period of sine curve functions) could not be determined separately for each image. This is a preliminary result of using 3D straight lines in bundle equations.

With the proposed method, additional parameters can be estimated without using more control points than needed for defining a datum. It makes the use of the sensor more efficient in practice.

Our further research will be on the problem of the First Order Design (FOD) for panoramic cameras. We are also interested in 3D object reconstruction using panoramic cameras.

ACKNOWLEDGEMENTS

REFERENCES

Amiri Parian, J. and Gruen, A., 2003. A Sensor Model for Panoramic Cameras. In Gruen/Kahmen (Eds.), 6th Conference on Optical 3D Measurement Techniques, Zurich, Switzerland, Vol. 2, pp. 130-141.

Amiri Parian, J. and Gruen, A., 2004a. A Refined Sensor Model for Panoramic Cameras. International Archives of Photogrammetry, Remote Sensing and Spatial Information Sciences, Vol. XXXIV, part 5/W16. ISPRS "Panoramic Photogrammetry Workshop", Dresden, Germany, 19-22 February 2004. http://www.commission5.isprs.org/wg1/workshop_pano/

Amiri Parian, J. and Gruen, A., 2004b. An Advanced Sensor Model for Panoramic Cameras, The XXth ISPRS International Archives of the Photogrammetry, Remote Sensing and Spatial Information Sciences, In: Proceedings of the XXth ISPRS Congress, Istanbul, July 2004, XXXV (B5), pp. 24-29.

Brown, D. C., 1971. Close range camera calibration, Journal of Photogrammetric Engineering & Remote Sensing, volume 37, No. 8, pp. 855-866.

Habib, A., Morgan, M., Kim, E. M. and Cheng, R., 2004. Linear Features in Photogrammetric Activities, XXth ISPRS Congress, PS ICWG II/IV: Automated Geo-Spatial Data Production and Updating, Istanbul, Turkey, 2004, pp. 610-615.

Habib, A., Asmamaw, A., Kelley, D. May, M., 2000. Linear Features in Photogrammetry, Report No. 450, Geodetic Science and Surveying, Department of Civil and Environmental Engineering and Geodetic Science, The Ohio State University, January 2000.

Hell, G., 1979. Terrestrische Bildtriangulation mit Beruecksichtigung zusaetzlicher Beobachtungen. DGK, Reihe C, Heft 252, Munchen.

Heuvel, F.A. van den, 1999. Estimation of interior orientation parameters from constraints on line measurements in a single image. Proceedings of International Archives of Photogrammetry and Remote Sensing, 32 (5W11), pp. 81-88.

Kager, H. and Kraus, K., 1976. Geowissenschaftliche Mitteilungen. XIII. Internationale Kongress fuer Photogrammetrie, Helsinki 1976.

Matthias, H., 1961. Umfassende Behandlung der Theodolitach-senfehler auf vektorieller Grundlage unter spezieller Berücksic-htigung der Taumelfehler der Kippachse. Verlag Leemann, Zürich.

Scheibe, K., Korsitzky, H., Reulke, R., Scheele, M. and Solbrig, M., 2001. EYESCAN - A High Resolution Digital Panoramic Camera. Robot Vision: International Workshop RobVis 2001, Auckland, New Zealand, Volume 1998, pp. 77-83.

Schneider, D. and Maas, H.-G., 2003. Geometric modeling and calibration of a high resolution panoramic camera. In Gruen/Kahmen (Eds.), 6th Conference on Optical 3D Measurement Techniques, Zurich, Switzerland, Vol. 2, pp. 122-129.

Schneider, D. and Maas, H.-G., 2004. Application of a geometrical model for panoramic image data. International Archives of Photogrammetry, Remote Sensing and Spatial Information Sciences, Vol. XXXIV, part 5/W16. ISPRS "Panoramic Photogrammetry Workshop", Dresden, Germany, 19-22 February 2004. http://www.commission5.isprs.org/wg1/workshop_pano/